

INSIGHTS INTO THE THERMOELECTRIC PROPERTIES OF P-TYPE FLUOROPEROVSKITE  $\text{AlZnF}_3$ Mudasir Younis Sofi<sup>1\*</sup>, Arshid Ahmad<sup>2</sup> and Shabir Ahmad Mir<sup>3</sup><sup>1</sup>Department of Physics, Jamia Millia Islamia, New Delhi-110025<sup>2</sup>Department of Physics, Indian Institute of Technology, New Delhi-122010<sup>3</sup>Condensed Matter Theory Group, School of Studies in Physics, Jiwaji University Gwalior, 474011 (India)**ABSTRACT**

Computer controlled simulations within the framework of density functional theory (DFT) have been employed to scrutinize the structural and thermoelectric properties of halide fluoroperovskite,  $\text{AlZnF}_3$ . The calculation of cohesive energy has been undertaken to examine the thermodynamic stability of the given material. The thermoelectric coefficients of the present material were investigated using the semi-classical Boltzmann theory as implemented in the BoltzTraP code. This material appears to be an excellent prospect for thermoelectric applications at both low and high temperatures based on the high values obtained from its Seebeck coefficient and figure of merit ( $Z_eT$ ), respectively.

*Keyword; Fluoroperovskites, Cohesive energy, Charge density, Thermoelectric properties*

**1. INTRODUCTION**

$\text{ABF}_3$  fluoroperovskites have piqued the interest of researchers in recent years due to their cubic phase stability and significant industrial implications [1,2]. They have exceptional properties such as magneto-resistance, ferromagnetism, photoluminescence, and thermoelectricity [3,4], and have been used for a variety of applications, including power storage, semiconductors, optical applications, magnetic tunnel junctions, and lenses [5,6]. Among other distinctive features, fluoroperovskites are regarded as appealing TE materials due to their fascinating electronic structures with both wide and narrow semiconducting band gaps [7]. Also, most fluoroperovskites are dynamically stable, as demonstrated by Roekeghem et al. [8] in phonon simulations of roughly 400 semiconductors and fluoroperovskites at fixed temperatures. The family of fluoroperovskites has sparked a great deal of attention in recent times because of their possible thermoelectric uses [9,10]. TE materials are intended to tackle burgeoning energy demands and lessen our dependence on fossil fuels by allowing direct heat-to-electricity conversion. The applicability of a material to thermoelectric technology is administered by a dimensionless figure of merit  $ZT = \frac{S^2\sigma}{k}T$ , where  $S$ ,  $\sigma$ ,  $k$  signifies the Seebeck coefficient, electrical conductivity, and thermal conductivity, respectively. For practical applications of materials in thermoelectrics,  $ZT \geq 1$ .

In the present article, we report a comprehensive assessment of the intermolecular stability, charge density behaviour and thermoelectric properties of potential fluoroperovskite  $\text{AlZnF}_3$ . The magnetic phase stability and electronic properties of this material are previously documented by A. Habib et al. [11]; however, till now, no theoretical investigation has been undertaken to investigate its possible thermoelectric properties. We therefore employed DFT-based calculations to get insights into the thermoelectric response of  $\text{AlZnF}_3$  fluoroperovskite.

**2. Computational Details**

The present simulations were carried out using the first – principles full potential linearized augmented plane – wave (FP-LAPW) method [12], in which the crystal space is divided into non-overlapping muffin tin spheres with atomic like wave functions and interstitial spaces subjected to plane wave basis set for eigen value convergence. To integrate the Brillouin zone, we employed a compact mesh of 2000-k points. The energy difference between the core and valence states is set to -6.0 Ry. The cut off variable  $R_{\text{MT}}K_{\text{max}} = 7$  Ry, where  $K_{\text{max}}$  is the reciprocal lattice vector and  $R_{\text{MT}}$  displays the MT sphere radii, was used to govern convergence. The cumulative charge difference between the two subsequent interactions was calibrated to less than  $10^{-4}$  e/a.u.<sup>3</sup> and the convergence criteria for energy was fixed at  $10^{-4}$  Ry. The thermoelectric properties were analysed using the BoltzTraP code [13] as integrated with the Wien2k program. The calculations of transport coefficients were accomplished by employing a denser mesh of 100000-k points.

**3. Results And Discussion**

The predicted structural, electronic and thermoelectric properties of  $\text{AlZnF}_3$  perovskite are discussed in the sections given below;

### 3.1 Structural and Electronic Properties

The present material,  $\text{AlZnF}_3$ , belongs to the Pm-3m (221) space group, with Al atoms holding corner positions, Zn atoms claiming body centre positions, and F atoms clutching face centre spots, as shown in Figure 1(a). As per theoretical study of A. Habib et al. [11], this material displays non-magnetic (NM) cubic phase stability. Nevertheless, in this work, we further calculated the cohesive energy of the given material to guarantee its intermolecular stability by using the following equation;

$$E_{\text{coh}}^{\text{AlZnF}_3} = \frac{[\text{Al} + \text{Zn} + 3E_{\text{F}}] - E_{\text{Optimized}}}{5}$$

Here,  $E_{\text{coh}}^{\text{AlZnF}_3}$  signifies the cohesive energy per atom of a material. The  $E_{\text{Optimized}}$  has been taken from the total energy-volume calculations reported by A. Habib et al. [11]. Following the calculations, the total cohesive energy and the energy per atom of  $\text{AlZnF}_3$  compound has been determined to be 17.27 eV and 3.45 eV/atom, respectively. The positive value of the cohesive energy signifies that the atoms are firmly held within the lattice structure of this halide, thereby confirming the inter-atomic stability of the given material.

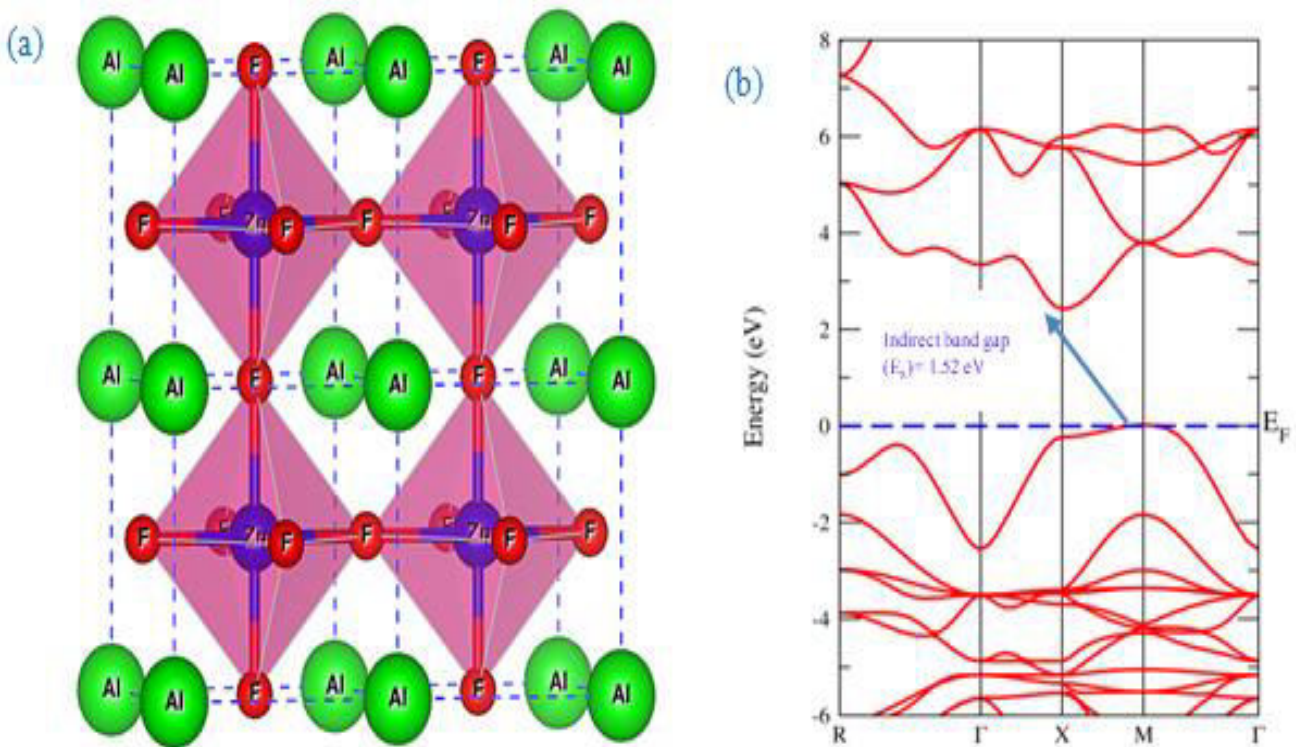


**Figure 1.** (a) Crystal structure of  $\text{AlZnF}_3$ ; (b) Band structure of  $\text{AlZnF}_3$  fluoroperovskite projected via GGA method.

The electronic profile of the given material has been previously investigated by A. Habib et al. [11], so here we only present a pictorial depiction of the band structure (BS) and density of states (DOS), as displayed in Figure 1(b) and Figure 2(a), respectively, to comprehend the band gap, as it is obligatory to explore the thermoelectric properties. After looking at BS and DOS, we can assert that the present material exhibits semi-conducting behaviour with an indirect band gap of  $\sim 2.40$  eV along X and M-symmetry points. These results are in line with those reported by A. Habib et al. [11], thereby validating our results. The semiconducting behaviour of this material with an indirect band gap prompted us to investigate its suitability for thermoelectric and solid-state device applications.

Furthermore, the electronic charge density plots were examined to investigate the bonding character of  $\text{AlZnF}_3$  fluoroperovskite along 011 planes, as shown in Figure 2(b). While examining the plot, it is clear that complete spherical contours surrounding Al atoms reflect an ionic bond between Al and F atoms; however, along Zn-F chain, sharing of electrons take place as is apparent from dumbbell shaped charge clouds between Zn and F atoms. The overall polar covalent bonding (mix of ionic and covalent) is preserved within the lattice structure of  $\text{AlZnF}_3$  compound, which benefits the thermoelectric response of this material.

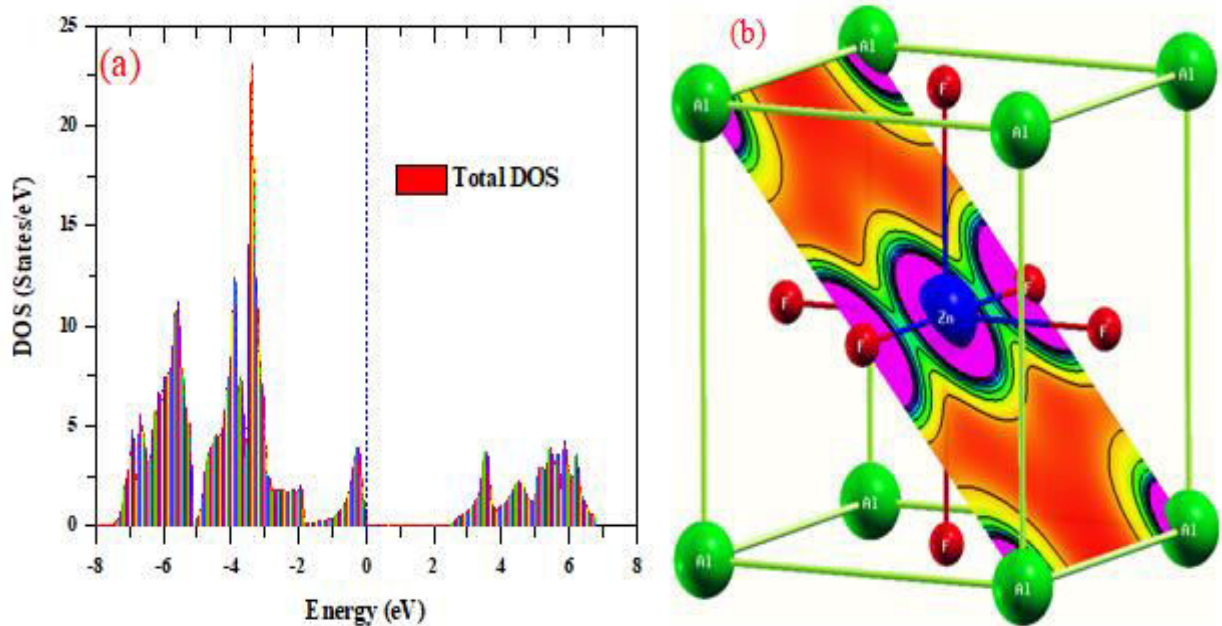


**Figure 2.** (a) Plot of the electronic density of states (DOS) calculated via GGA method; and (b) Charge density graphics of AlZnF<sub>3</sub> compound along 011 planes.

### 3.2 Thermoelectric Properties

The transport properties of the present material were explored using semi – classical Boltzmann theory implemented in the BoltzTraP code under constant relaxation time approximation ( $\tau = 0.5 \times 10^{-15}$  s). In this work, the chemical potential dependency of transport coefficients has been analysed at different temperatures and the obtained results are depicted in Figures 3(a-d). The chemical potential is an important factor in determining the charge carriers (electrons or holes) involved in transport phenomena. Moreover, the thermoelectric parameters, particularly the Seebeck coefficient, power factor and figure of merit (ZT) are significantly influenced by the value of the chemical potential. The term chemical potential can be defined as the quantity/amount of energy required to add or withdraw electrons from a system when coulomb repulsion exists. The inclusion or exclusion of electrons from a system result in a positive or negative chemical potential. As electrons are added to a system, the density of electrons grows, offering the system an n-type character; in contrast, as electrons are withdrawn from a system, the number of void spaces (also referred to as hole carriers) increases, granting the system a p-type character. Additionally, when looking at the electronic DOS of the given material, it is evident that the valence band has a greater number of accessible states than the conduction band, implying the presence of a substantial number of hole carriers and therefore supporting the predominant p-type nature of the studied material.

Herein, we have examined the variation of Seebeck coefficient (S), electrical conductivity( $\sigma/\tau$ ), electronic thermal conductivity ( $K_e/\tau$ ), and figure of merit against chemical potential ( $-2.5 \leq \mu \leq 4.5$ ) at different temperatures, and all of these parameters are debated below;

Seebeck coefficient (S) is defined as the ability of a material to generate induced emf when a temperature differential is applied and is given as;  $S = \frac{\Delta V}{\Delta T}$ , where  $\Delta T$  characterizes the temperature gradient. The Seebeck coefficient for the given material at various Kelvin temperatures against chemical potential is displayed in Figure 3(a); it is evident that throughout the entire chemical potential range, the Seebeck coefficient exhibits different peaks and slopes. The (n)p-type region of the chemical potential exhibits the highest value of 3000  $\mu V/K^{-1}$ . The given compound presents higher Seebeck coefficient value as a consequence of the wide band gap and confined carrier mobility. Nevertheless, S is slightly lowered to 1200  $\mu V/K^{-1}$  at higher temperatures. The decrease in Seebeck coefficient at higher temperatures is driven by the bipolar effect, which persists when bound electrons are boosted by thermal energy and form electron-hole pairs. These results are exclusively in conformity with the Mott relation, which quantifies the Seebeck coefficient's dependency on chemical potential and temperature and is stated as [14];  $S = \frac{\pi^2 k_B^2 T}{3e} \left\{ \frac{1}{n} \frac{dn(\epsilon)}{d\epsilon} + \frac{1}{\mu} \frac{dn(\epsilon)}{d\epsilon} \right\}_{\epsilon=\mu}$ .

The present material exhibits non-zero value of S at elevated temperatures; therefore, it has the potential to be used in thermoelectric coolers, thermoelectric generators, temperature sensors, and thermocouples.

Electrical conductivity ( $\sigma/\tau$ ) defines the ability of a substance to carry electric currents triggered by positive and negative charges. Figure 3(b) conveys the pictorial depiction of electrical conductivity at different temperatures in response to chemical potential. Given that there is a wide band gap, it is quite likely that the material will have relatively low electrical conductivity. Moreover, from Figure 3(b), the electrical conductivity ceases at  $\mu=0$  because the absence of energy bands in the region renders the Fermi level destitute of charge carriers. The (n)p-type doping zone at 300 K has the highest value of  $2.25 \times 10^{20} (\Omega^{-1}\text{m}^{-1}\text{s}^{-1})$ .

The quantity of heat that flows from electron mobility ( $K_e$ ) and lattice vibration ( $K_{ph}$ ) is characterised as thermal conductivity. In this study, we focused primarily on the electronic thermal conductivity and disregarded the thermal conductivity of phonons ( $K_{ph}$ ) since it is outside the scope of the BoltzTraP code. The variation of electronic thermal conductivity ( $K_e/\tau$ ) against chemical potential at various temperatures is shown in Figure 3(c). The  $K_e$  increases with increasing temperature because raising the temperature elevates the carrier mobility which enhances the electronic movement and thereby increases the electronic thermal conductivity. The temperature-dependent change of  $\sigma$  and  $K_e$  exhibits the same behaviour since they are interrelated by Wiedemann Franz Law  $K_e=L\sigma T$ . At 300 K, the obtained value of ( $K_e/\tau$ ) is  $1.5 \times 10^{15} (\text{Wm}^{-1}\text{K}^{-1}\text{s}^{-1})$  in (n)p-doping region, which is comparatively low, hence favouring the better TE performance of AlZnF<sub>3</sub> fluoroperovskite.

Having all of these parameters in hand, we can finally assess true competency of this material by computing the figure of merit ( $Z_e T$ ) as  $ZT$ , in real sense gauges the fittingness of a material for thermoelectric technology. Thermoelectric devices are assumed to make effective use of materials with higher  $ZT$  values as they have greater heat-to-electricity conversion efficiency. The graphical variation of electronic figure of merit ( $Z_e T$ ) for AlZnF<sub>3</sub> is portrayed in Figure 3(d). As one can see, the maximum value of  $Z_e T$  at 300 K is 1.01, which is certainly more than unity. The high  $ZT$  value opens up the possibility for this material to have potential waste heat recovery applications in thermoelectric technology.

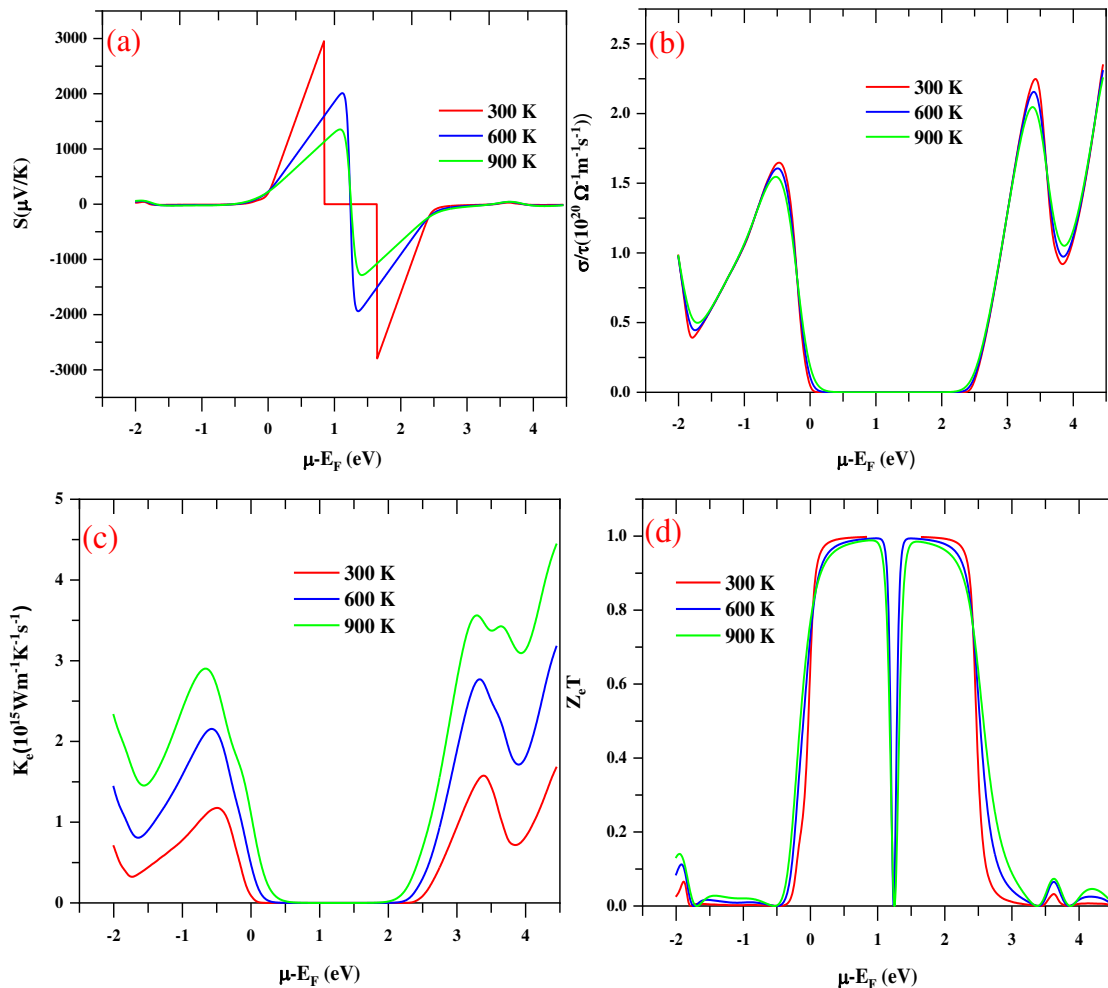


**Figure 3.** Thermoelectric coefficients of AlZnF<sub>3</sub> (a) Seeback Coefficient (S); (b) electrical conductivity ( $\sigma/\tau$ ); (c) electronic thermal conductivity ( $K_e/\tau$ ); (d) figure of merit ( $Z_e T$ ) at different temperatures (300 K, 600 K and 900 K).

#### 4. CONCLUSIONS

The first principles approach was effectively used to analyse the structural stability and thermoelectric properties of the potential fluoroperovskite  $\text{AlZnF}_3$ . The positive cohesive energy confirmed the interatomic stability of the given material. The electronic structure unveiled the wide band gap semiconducting character of the studied material. The charge density behaviour suggests polar covalent bonding, facilitating thermoelectric exploration of this material. The thermoelectric investigation found higher values of Seebeck and figure of merit, unlocking avenues for this material to have robust applications in thermometric technology.

#### REFERENCES

1. S. Bouhmaidi, A. Marjaoui, A. Talbi, M. Zanouni, K. Nouneh, L. Settia, *Computational Condensed Matter* 31, 2022, e00663.
2. M. Reda Kabli, J. Rehman, M. Bilal, T. Muhammad Usman, A. Mahmood Ali, K. Shahzad, *Physics Letters A* 412, 7 2021, 127574
3. M. Sohail, M. Husain, N. Rahman, K. Althubeiti, M. Algethami, A. Ali Khan, A. Iqbal, A. Ullah, A. Khan and R. Khan, *RSC Adv.*, 2022, 12, 7002-7008.
4. R. Arar T. Ouahrani, D. Varshney R. Khenata, G. Murtaza, D. Rached A. Bouhemadou Y. Al-Douri, S. Bin Omran A.H. Reshak, *Materials Science in Semiconductor Processing* 33, 2015, 127-135.
5. C. Dotzler, G.V.M. Williams, and A. Edgar, *Curr. Appl. Phys.* 8, 44 (2008).
6. A.A. Mubarak and A.A. Mousa, *Comput. Mater. Sci.* 59, 6 (2012).
7. Asad Ali, Altaf Ur Rahman, and Gul Rahman, *Physica B: Condensed Matter*, 565, 15 2019, 18-24.
8. A.V. Roekeghem, J. Carrete, C. Oses, S. Curtarolo, N. Mingo, *Phys. Rev. X.* 6 (2016) 014061.
9. R. Ullah, Ali H. Reshak, M. Azmat Ali, A. Khan, Ghulam Murtaza, Murefahmana AL-Anazy, H. Althib, Tahani H. Flemban, *Int J. Energy Res.* 2021;45:8711–8723.
10. Y. Selmani, H. Labrima, S. Ziti, L. Bahmada, *Computational Condensed Matter*, 32, 2022, e00699
11. A. Habib, M. Husain, M. Sajjad, N. Rahman, R. Khan, M. Sohail, I. Hassan Ali, S. Iqbal, M. Ilyas Khan, Sara A. M. Ebraheem, Ahmed M. El-Sabrou, and Hosam O. Elansary, *Materials* 2022, 15, 2669.
12. Schwarz, K., Blaha, P. & Madsen, G. K. H. Electronic structure calculations of solids using the WIEN2k package for material sciences. *Comput. Phys. Commun.* 147(1–2), 71–76 (2002).
13. Madsen, G. K. H. & Singh, D. J. BoltzTraP. A code for calculating band-structure dependent quantities. *Comput. Phys. Commun.* 175(1), 67–71 (2006).
14. M. Jonson and G. D. Mahan, *Phys. Rev. B*, 1980, 21, 4223–4229.